Aalborg Universitet

Multi-objective co-optimization of power and heat in urban areas considering local air pollution

Golmohamadi, Hessam; Keypour, Reza; Mirzazade, Pouya

Full Length Article

Multi-objective co-optimization of power and heat in urban areas considering local air pollution

Check for updates

Hessam Golmohamadi [a], Reza Keypour [b,*], Pouya Mirzazade [b]

[a] Department of Computer Science, Aalborg University, 9220 Aalborg, Denmark
[b] Faculty of Electrical and Computer Engineering, Semnan University, Semnan, Iran

A B S T R A C T

This paper suggests a novel framework to co-optimize the power and heat in smart cities considering the local air pollution from energy generation units and traffic fumes. To achieve the aim, a smart city comprised of power and heat generation units is addressed. The energy system of the smart city can be connected to the main grid or be operated as a stand-alone power system. Connecting to the main grid, the city trades power in the wholesale electricity market with price uncertainty. In order to co-optimize the operation cost of energy units and to control the pollution levels of the urban area, a Combined Economic Pollution Dispatch Problem (CEPDP) is developed. The CEPDP is optimized under air pollution constraints from both energy generation units and traffic fumes. Increasing the applicability of the suggested approach, pollution density is addressed using the Box model while the wind speed and surface roughness influence on it. To solve the CEPDP, a multi-objective Non-Dominated Sorting Genetic Algorithm (NSGA II) is proposed. The suggested approach is implemented in a virtually-designed smart city located in the center of Iran. The results show that although the use of distributed generation decreases the global emission all over the world, it transmits the air pollution from suburban areas to cities increasing the local pollution. The two conflict objectives, i.e. global and local pollutions, may change the operation of distributed generation to meet the local environment requirements of cities.

© 2020 Karabuk University. Publishing services by Elsevier B.V. This is an open access article under the CC BY-NC-ND license (http://creativecommons.org/licenses/by-nc-nd/4.0/).

1. Introduction

1.1. Problem description

Recently, the penetration of Distributed Generation (DG) has been increased in power systems all over the world [1]. From the viewpoint of energy generation, the DGs take advantage of cost and reliability. In contrast, from the viewpoint of air pollution, urban power generation increases local sulfur/carbon dioxide emissions in urban areas. Therefore, the major challenge is that when the DGs are substituted for the large-scale power generators, the pollution is transmitted from suburban areas to cities. It is confirmed that DG exploitation decreases global emission [2]. But from the viewpoint of urban pollution, the DG operation increases the local pollution in urban areas. The situation may be deteriorated in large cities with high traffic fumes. As a result, the DG deployment decreases the global emission and increases the local

pollution in some time durations. In fact, global and local pollutions are two conflict objectives that should be more studied. As a result, it will lead to severe pollution problems which can damage the inhabitants' health seriously. Consequently, bringing DGs to the cities without emission control puts the health of people at risk. It is evident that the emission control may deviate the energy dispatch problem from optimum points. It is interpreted as the cost of local pollution control for cities. Therefore, energy optimization in cities without local pollution control may fail to be applicable in reality. To meet the challenge, the local pollution constraints should be incorporated into the energy management problem of urban areas.

1.2. Literature review

The urban supply systems are normally comprised of renewable energy resources, conventional thermal/heat generation units, storage devices, and a number of loads with a two-way communication system [3]. In a smart city, when local energy generation, i.e. power and heat, is more than local consumption, the city can sell the surplus of energy to the main grid as a wholesale market par-

ticipant. Adversely, if the local generation cannot meet the local demand, the city purchase deficit of energy from the main grid [4].

Considering the DGs, Economic Load Dispatch (ELD) is an essential task not only in current power systems but also in future smart cities with higher DG penetration. The ELD aims to optimize power flow in power networks at minimum fuel cost. The ELD can be in various forms including Convex Economic Dispatch (CED), Non-Convex Economic Dispatch (NCED), Economic Emission Dispatch (EED), Emission constrained Economic Dispatch (ECED), and Combined Economic Emission Dispatch (CEED). To solve the ELD problem, two kinds of solution methodologies are used in the literature as (1) mathematical optimization approaches (2) heuristic methodologies. Regarding the mathematical approaches, Linear Programming (LP) [5], Non-Linear Programming (NLP) [6], Mixed Integer Linear Programming (MILP) [7] and Dynamic Programming (DP) [8] were addressed traditionally from 1995 to 2007. On the other hand, due to the non-linearity of the problems and poor convergence of some mathematical approaches, heuristic methods have been developed shortly afterward. In this way, Genetic Algorithm (GA) [9], Simulated Annealing (SA) [10], Ant Colony (AC) [11], Particle Swarm Optimization (PSO) [12], Harmony Search Algorithm (HSA) [13] and Gravitational Search Algorithm (GSA) [14] were developed from 2008 to 2017.

Incorporating emission control into the ELD, the Economic Emission Dispatch Problem (EEDP) is subjected to further researches. As a result, the EEDP is a crucial problem for power companies. The problem is comprised of cost and emission minimization. Increasing the penetration of DGs in cities, the operation of generation systems has been restricted to reduce air pollution in the environment. In China, a research study was conducted to optimize EEDP proposing ensemble multi-objective differential evolution (EMODE) [15]. In [16], the EEDP is optimized using the Adaptive Wind Driven Optimization (AWDO) algorithm. Comparing the results with the other heuristic methods, the results confirm that AWDO outperforms the other tested algorithms. A robust-based optimization approach is suggested in [17] to optimize the EEDP considering the uncertainties associated with renewable energy resources. In [18] a recurrent neural network (RNN) is proposed to solve the EEDP. Two binary variables are used to split the feasible region of the approach into convex areas. In paper [19], a combined heat and power (CHP) system is proposed to optimize the power and heat consumption in a district heating system. The model aims to hedge against the volatility of wind energy in the power system.

In paper [20], heat storage of distribution pipelines is formulated. Moreover, in order to address the uncertainty of wind energy resources, a robust model is incorporated into the problem. In [21], the dual-objective EEDP is solved using Flower Pollination Algorithm (FPA). The results show that the proposed FPA approach has many advantages against the other swarm intelligence algorithms for various power systems, even for large scale power systems. A novel structure for the dynamic EEDP is proposed in [22] using bi-level robust optimization in a power system with wind power penetration. The problem is solved using teaching-learning-based optimization (TLBO) algorithm and linear programming (LP).

In 2018, a dynamic EEDP is constructed considering the uncertain nature of wind power output [23]. The study proposes a hybrid multi-objective algorithm that integrates differential evolution and PSO algorithm to solve the approach. In addition, a workable study is conducted in the Taiwan Power Company system to optimize the EEDP by integrating simulated annealing and the interactive best-compromise approach [24]. In 2019, a novel EEDP is suggested including Plug-in Electric Vehicles (PEVs) for peak shaving and valley filling [25]. Following a similar pattern, the research study [26]

proposes the EEDP incorporating a novel structure to identify the fleet size capability of a power network.

Air pollution includes any type of material that enters the air in certain quantities and has significant effects on health, welfare, or the environment. Air pollutants are classified into three categories in terms of the radius of effect: local, regional, and global. Pollutants with local effects, with a relatively lower radius of effect, are the particles smaller than 10 μm (CO, PM-10, and NO_x). Pollutants with regional impact are NO_x and SO_2. The only pollutant that has a global effect is CO_2 which causes global climate change. The term *"pollution"* is usually used for local and regional pollutants, and the term *"emission"* is used for global pollutants.

In the literature, most research studies have concentrated on emission. Paper [27] investigates CO_2 emissions from the electricity generation sector. In [2], new trajectories of optimal technology adoption are established to reduce the cost of CO_2 emission. The effects of CO_2 emission and local pollutant emission taxes on joint transmission-generation expansion planning are analyzed in [28]. A research study has investigated the economic dispatch of CHP units to minimize the total operational cost and emissions of the pollutant gases [29]. In [30], a stochastic multi-objective optimization approach is suggested as an economic/emission dispatch problem. The study uses stochastic programming to cover the uncertainties associated with demand and the environment. In continue, the neural network is addressed as the optimization solution for the economic dispatch of a CHP [31]. A recent study suggests an efficient fitness-based differential evolution algorithm for dynamic economic emission dispatch problem [32]. This paper compares the proposed approach with conventional single-objective and multi-objective optimization problems. In [33], a modified harmony search algorithm is addressed to optimize the combined economic emission dispatch problem of the microgrid in the presence of wind turbines.

In order to clarify the contribution of the suggested problem, Table 1 makes a comparison between the current study and 5 recent studies.

1.3. Paper contributions and organization

As Table 1 reveals, most of the research studies were conducted considering the global emission. It is confirmed that the use of distributed generations and CHPs, decreases global emission all over the world. But it increases the local pollution in urban areas. This paper aims to narrow this gap by optimizing the EEDP addressing local pollution instead of global emission. This is an original idea that is not examined in previous studies, to the best of our knowledge. Moreover, despite the local pollution emitted from generation units, the impacts of traffic fumes in the urban areas are studied concurrently. Also, the impacts of electricity price uncertainty on the trading strategies of the city are investigated.

Therefore, a multi-objective approach about the Combined Economic Pollution Dispatch Problem (CEPDP) of an urban area is proposed. The main aim is to solve the problem considering both the operation cost and the pollution function of the generation units. Considering the operation cost, the cost function of generation units, including power-only units, heat-only units, and cogeneration units, plus the procurement cost from the electricity market is addressed. Note that the electricity price of the electricity market is considered as the main uncertainty; therefore, the Time-series-based Auto-Regressive Integrated Moving Average (ARIMA) approach is used to consider every possible scenario of electricity price. Regarding the pollution control, the pollution density from generation units and traffic fumes are incorporated into the Box model while the wind speed and surface roughness influence on it. Finally, the non-linear multi-objective CEPDP is solved using the Non-Dominated Sorting Genetic Algorithm (NSGA II). There-

Table 1
A brief comparison between the suggested approach and some recent studies.

Reference	Environmental Factor		Energy Generation Units			Uncertainty
	Global Emission	Local Pollution	CHP	Heat-only	Power-only	
[2]	X		X	X		Not addressed
[28]		X			X	Not addressed
[30]	X		X	X	X	Demand
[31]	X		X	X		Not addressed
[32]		X	X	X		Not addressed
Current Study		X	X	X	X	Electricity Price

fore, the main contributions to the proposed approach can be stated as follows:

(1) Formulating the CEPDP for urban areas addressing local pollution instead of conventional global emission.
(2) Incorporating the Box model into the CEPDP to study the impact of the wind regime on local pollution.

The remainder of this paper is organized as follows. Section 2 provides the mathematical formulation of the proposed approach in terms of the objective function, problem constraints, and solution methodology. Section 3 is devoted to simulations and discussions. The conclusion of the paper is presented in Section 4. The appendix of the study is stated in Appendix.

2. Problem formulation

In this paper, a smart city with power-only units, CHP units, and heat-only units are modeled. The objective function of the proposed multi-objective approach is comprised of three terms including cost minimization, pollution minimization, and maximization of energy generation considering three different types of generation units. Consequently, the multi-objective structure of the CEPDP is formulated as follows:

$$Min\left[F_{Operation}^{Cost}(t) + F_{Generation}^{Pollution}(t)\right] \tag{1}$$

where F^{Cost} demonstrates the total operation cost of the city, including operation cost of all generation units plus the procurement cost from the electricity market. $F^{Pollution}$ is the pollution function of the generation units.

2.1. Objective function

The objective function of the CEPDP comprises the simultaneous minimization of operational cost and pollution. The operational cost function of the city is stated as follows:

$$F_{Operation}^{Cost}(t) = \sum_{i=1}^{Ni} F_{TH}^i(t) + \sum_{j=1}^{Nj} F_{CHP}^j(t) + \sum_{k=1}^{Nh} F_{HS}^k(t) + F_{Grid}(t) \tag{2}$$

where F^{Cost} is the total operational cost function of the city, F_{TH} is the operational cost of power-only units, F_{CHP} is the operational cost of CHP units, F_{HS} is the operational cost of heat-only units and F_{Grid} is the procurement cost from the main grid. In addition, N_i describes the number of power-only units, N_j is the number of CHP units and N_h is the number of heat-only units. In this way, i, j, and k are the indices of power-only, CHP, and heat-only units, respectively. Note that the city can purchase a deficit of its electrical power from the main grid ($F_{Grid} > 0$) in connected mode and/or sell the surplus of electrical power to the main grid ($F_{Grid} < 0$) in islanded mode.

The first term in the objective function, i.e. Eq. (2), describes the operational cost of thermal power generation units. A detailed formulation of the operational cost can be stated as follows [34]:

$$F_{TH}^i(t) = (a_{TH}^i) + \left(b_{TH}^i \times P_{TH}^i(t)\right) + \left(c_{TH}^i \times P_{TH}^{i2}(t)\right)$$
$$+ \left|d_{TH}^i \times \sin\left[e_{TH}^i \times (P_{TH,\ min}^i(t) - P_{TH}^i(t))\right]\right| \tag{3}$$

where a_{TH}, b_{TH}, c_{TH}, d_{TH}, and e_{TH} are the cost coefficients of thermal unit i. P_{TH}^i and $P_{TH,min}^i$ are the power generation and minimum power generation of thermal unit i, respectively.

Note that the fuel cost function of the generation units is addressed considering the valve-point effects. In fact, the sinusoidal term in Eq. (3) describes the valve-point effect which practically appears when the steam admission valve starts to open.

The second term in Eq. (2) demonstrates the operation cost of combined heat and power generation as follows [35]:

$$F_{CHP}^j(t) = \left[a_{CHP}^j + b_{CHP}^j \times P_{CHP}^j(t) + c_{CHP}^j \times P_{CHP}^j(t)^2\right]$$
$$+ \left[d_{CHP}^j \times H_{CHP}^j(t) + e_{CHP}^j \times H_{CHP}^j(t)^2\right]$$
$$+ \left[f_{CHP}^i \times P_{CHP}^j(t) \times H_{CHP}^j(t)\right] \tag{4}$$

where a_{CHP}, b_{CHP}, c_{CHP}, d_{CHP}, e_{CHP} and f_{CHP} are the cost coefficients of CHP unit j. P_{CHP}^j and H_{CHP}^j are power and heat generation of CHP unit j, respectively.

The third term in Eq. (2) shows the operational cost of heat-only generation units. Heat-Only generation units produce thermal energy in different forms for use in district heating applications. Unlike the CHP units which produce thermal energy as a by-product of electricity generation, heat-only generation units are dedicated to heat generation. The cost function of a heat-only generation unit can be expressed as follows [36]:

$$F_{HS}(t) = a_{HS}^k + b_{HS}^k \times H_{HS}^k(t) + c_{HS}^k \times \left(H_{HS}^k(t)\right)^2 \tag{5}$$

where a_{HS}, b_{HS} and c_{HS} are the cost coefficients of heat generation unit k. H_{HS}^k denotes the heat output of unit k.

The last term in the objective function Eq. (2) indicates the cost of purchasing/selling energy from/to the electricity market of the main grid. Therefore, this cost is formulated as follows:

$$F_{Grid}(t) = \sum_{\omega=1}^{N_\omega} E_\omega\left[\lambda_{Grid}^t(\omega) \times P_{Grid}^t(\omega)\right] \tag{6}$$

here $P_{Grid}(\omega)$ is the power traded between electricity market and city for price scenario ω ($P_{grid} > 0$ when the city purchases energy and $P_{grid} < 0$ when the city sells energy to the main grid) and $\lambda_{grid}^t(\omega)$ is the electricity price scenario of the wholesale market in scenario ω during the period of t. Note that N_ω is the number of scenarios and E is the expectation operator.

In this paper, the electricity price is considered as a variable with imperfect data. Therefore, in order to consider all possible realizations of the electricity price, a scenario generation scheme is used. Considering the cost function Eq. (6), the city can participate in the electricity market with imperfect information about the electricity price. In fact, the uncertain and volatile nature of the electricity price affects the operation scheduling of the city.

Obviously, the operators of the city should decide on the operational scheduling considering different scenarios of electricity prices in the main grid.

The second term in the objective function Eq. (1) describes the pollution function of the CEPDP. The pollution function of the city comprises the pollution functions of power-only units, CHP units, and heat-only generation units. In this way, the most important pollutions considered in the power system studies, due to their impacts on the environment, are SO_2, CO_2, and NO_x which are modeled technically by the polynomial functions for the SO_2 pollution, emitted pollution in terms of ton per MW for the CO_2 and exponential function for the NO_x pollution. Consequently, the pollution functions of the generation resources of the city are described as follows [34]:

$$F_{Generation}^{Pollution}(t) = E_s(t) + E_c(t) \tag{7}$$

$$E_s(t) = \sum_{i=1}^{Ni} \left[\begin{array}{c} \alpha_{TH}^i + \left(\beta_{TH}^i \times P_{TH}^i \right) + \left(\gamma_{TH}^i \times P_{TH}^i(t)^2 \right) \\ + \zeta_{TH}^i \times \left(e^{\lambda_{TH}^i \cdot P_{TH}^i} \right) \end{array} \right]$$
$$+ \sum_{j=1}^{Nj} \left[\left(\theta_{CHP}^j + \eta_{CHP}^j \right) \times P_{CHP}^j(t) \right] + \sum_{k=1}^{Nk} \left[\left(\pi_{HS}^k + \rho_{HS}^k \right) \times H_{HS}^k(t) \right] \tag{8}$$

$$E_c(t) = \sum_{i=1}^{Ni} \tau_{TH}^i . P_{TH}^i + \sum_{j=1}^{Nj} \psi_{CHP}^j P_{CHP}^j + \sum_{k=1}^{Nk} \sigma_{HS}^k H_{HS}^k \tag{9}$$

where E_s describes the pollution function for SO_2 and NO_x pollutions. Moreover, E_c indicates the pollution function for CO_2 pollution. α, β, γ, ζ and λ are the pollution coefficients for power-only units, η and θ are the pollution coefficients for CHP units, π and ρ are the pollution coefficients for heat-only units. Moreover, τ, ψ, and σ denote the coefficients of CO_2 pollution for generation units.

2.2. Problem constraints

The operational constraints of the city are modeled as follows:

$$\sum_{i=1}^{Ni} P_{TH}^i(t) + \sum_{j=1}^{Nj} P_{CHP}^j(t) + P_{Grid} = P_d \tag{10}$$

$$\sum_{k=1}^{Nk} H_{HS}^k(t) + \sum_{j=1}^{Nj} H_{CHP}^j(t) = H_d \tag{11}$$

$$P_{min}^i \leqslant P^i \leqslant P_{max}^i \tag{12}$$

$$H_{min}^k \leqslant H^k \leqslant H_{max}^k \tag{13}$$

$$P_{min}^j \leqslant P^j \leqslant P_{max}^j \tag{14}$$

$$H_{min}^j \leqslant H^j \leqslant H_{max}^j \tag{15}$$

Equality (10) ensures that during each operation period, the total production of power generation units, including power-only units and CHP units, plus the purchased/sold power from/to the main grid should be equal to the clients' electrical demand. Equality (11) enforces that the total production of heat generation units, including CHP units and heat-only units, must be equal to the heat demand of inhabitants. In this way, P_d and H_d are electrical and heat demands of the city. Inequalities (12)–(15) limit the power and heat generation of units, including power-only units, CHP units, and heat-only units within the maximum and minimum allowed capacity thresholds during all operation periods. In these constraints, P_{min}^i and P_{max}^i are minimum and maximum power output of power-only unit i, H_{min}^k and H_{max}^k are minimum and maximum heat output of heat-only unit k, P_{min}^i and P_{max}^i are minimum and maximum power output of CHP unit i, H_{min}^j and H_{max}^j are minimum and maximum heat output of CHP unit j.

Fig. 1 illustrates the power-heat Feasible Operation Range (FOR) of a CHP unit in terms of power and heat generation. The FOR of the CHP can be stated as a set of N_{Linear} linear inequality constraints as below [37]:

$$x^{j',j,t} \times H_{CHP}^j(t) + y^{j',j,t} \times P_{CHP}^j(t) \geqslant z^{j',j,t}$$
$$s.t. \left| \begin{array}{l} j' = 1, ..., N_{Linear} \\ j = 1, ..., N_j \end{array} \right. \tag{16}$$

As Fig. 1 reveals, the FOR is determined by the curve ABCDEF. The FOR shows the trend of heat (power) change with respect to the variation of power (heat) variable.

2.3. Local pollution of city

Due to the higher efficiency of DG systems and usage of wasted heat generated by the power-only units and CHP units, it is expected to observe a considerable reduction in pollution from generation resources in comparison to the state when heat and power are generated separately by boiler and power stations, respectively. The main challenge for this problem is that when DGs are substituted for the large-scale power generators, the pollution is transmitted from suburban areas to the urban areas: a pollution problem which can cause health problems for the urban residents. In order to prevent concentrating pollutants in the air of urban areas, the problem should be studied by considering the allowed pollution level. In this way, the operation of DGs may be affected by the local pollution level which depends heavily on the wind speed regime. Therefore, in order to satisfy the pollution constraints, the city operator may decrease the power-heat generation level of the units. As a result, the city may not be operated cost-effectively during the hours when the pollution level exceeds the upper threshold. In this situation, the city should procure the deficit of energy from the main grid to observe the local pollution constraints.

In this study, in order to incorporate the pollution from DGs and traffic fumes into the CEPDP, Box Method, as a deterministic air pollution method, is addressed evaluating the distribution of the air pollution in an urban area.

The box model is considered as the city area in which input and output pollutants are allowed.

In this method, the urban area is considered as a simple box with a specific space. The height of the box is the length of the atmosphere above the city which is affected by pollution. This height is usually within 60 to 100 m above the surface.
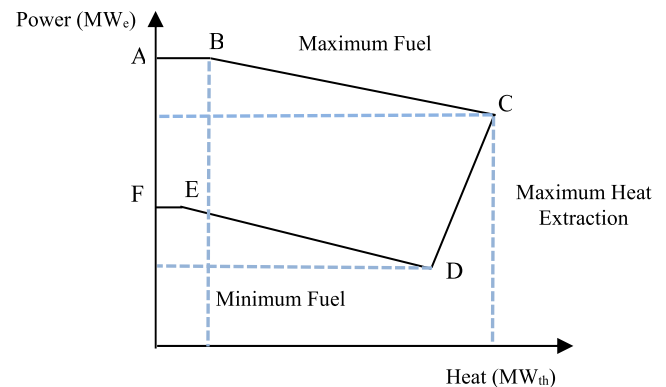

Fig. 1. Operation Range of Co-Generation Units.

The Box Model uses solutions of the diffusion equation. In this case, three-dimensional equations are addressed to better describe the pollutant movements in the city. Mathematically, the three-dimensional transfer-release equation in a transient state and orthogonal coordinate system can be stated as follows [27]:

$$\frac{\partial C}{\partial t} + u\frac{\partial C}{\partial x} + v\frac{\partial C}{\partial y} + w\frac{\partial C}{\partial z} = \frac{\partial}{\partial x}\left(k_x\frac{\partial C}{\partial x}\right) + \frac{\partial}{\partial y}\left(k_y\frac{\partial C}{\partial y}\right)$$
$$+ \frac{\partial}{\partial z}\left(k_z\frac{\partial C}{\partial z}\right) + Q \tag{17}$$

where C is the time-averaged concentration of pollution, x, y, z are the Cartesian coordinates, Q is the source of pollution (produced pollution), u, v, w are the components of the time-averaged wind velocity vector, k_x, k_y, k_z are the diffusion coefficients in the corresponding direction.

In order to simplify the diffusion Eq. (17), it is assumed that the wind velocity in y and z directions is negligible. Furthermore, pollutants' transmission through tubular molecular pollution in comparison to pollutants' transmission through wind flow is ignored, thus the following assumptions are applied:

$$\frac{\partial}{\partial x}\left(kz\frac{\partial C}{\partial x}\right) = 0 \tag{18}$$

$$\frac{\partial}{\partial y}\left(kz\frac{\partial C}{\partial y}\right) = 0 \tag{19}$$

In order to implement the general box model, i.e. Eqs. (17)–(19), the diffusion equation for local pollution is rewritten based on the mathematical notation of the suggested approach. Therefore, the diffusion equation of the city can be restated as follows:

$$F_{Local}^{Pollution}(t) - F_{Local}^{Pollution}(t-1) = F_{Traffic}^{Pollution} + F_{Generation}^{Pollution}(t)$$
$$- \frac{V_{Wind}(t) \times \left(F_{Inlet}^{Pollution}(t) - F_{Outlet}^{Pollution}(t)\right)}{G_{Local}} \tag{20}$$

$$F_{Local}^{Pollution}(t) \leqslant F_{Local}^{Pollution,Max} \tag{21}$$

where V_{Wind} is wind velocity, $F_{Local}^{Pollution}(t)$ and $F_{Local}^{Pollution}(t-1)$ are concentrations of local pollutants in two successive times, $F_{Generation}^{Pollution}(t)$ is pollution generation, $F_{Inlet}^{Pollution}(t)$ and $F_{Outlet}^{Pollution}(t)$ are the amounts of inlet and outlet of pollution in the control volume, respectively, $F_{Traffic}^{Pollution}(t)$ is the pollution from traffic volumes of cars and $F_{Local}^{Pollution,Max}$ is the maximum allowed threshold of pollution according to different standards. Note that the coefficient G_{loc} is a function of city shape and natural barriers like mountains and buildings.
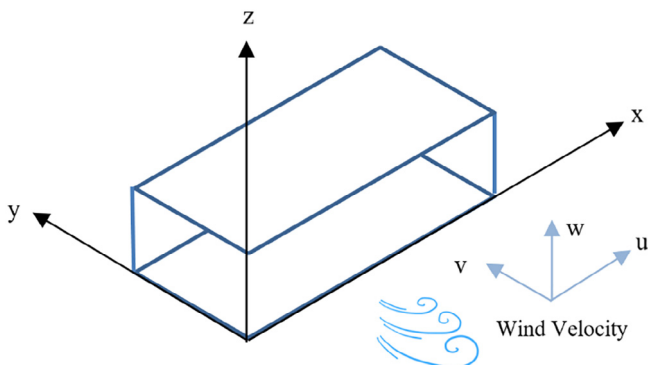
Fig. 2 shows a schematic diagram about the Box model of air pollution in the city.

To provide a general overview of the suggested approach, Fig. 3 illustrates the incorporation of the Box Model into the CEPDP. Based on the figure, the local air pollution of the urban area is addressed as a box model. In this model, the inlet pollution, i.e. $F_{Inlet}^{Pollution}(t)$, is imported to the city from suburban areas. The outlet pollution is modeled by $F_{Outlet}^{Pollution}(t)$ which is exported from the city to suburban areas. The inlet and outlet pollutions are affected by the wind regime. Despite the inlet and outlet pollution, there are three types of energy generation units, including CHP, power-only units, and heat-only units, which generate local pollution. Moreover, the patterns of local pollution from traffic fumes are simulated. The city can purchase/sell the deficit/excess of power generation from the main grid. It worth mentioning that the traffic fumes, i.e. $F_{Traffic}^{Pollution}(t)$, is considered as input perfect data. The data of traffic fume is extracted from the local meteorological office.

2.4. Solution methodology

Optimizing multi-objective functions, a specific methodology is required to find the best solution from the Pareto front. In the literature, many solution methodologies are suggested. Among them, the min-max method [35] and fuzzy-Pareto-dominance [36] are the most common methods. Recently, evolutionary algorithms have attracted much attention in finding optimal solutions. In this study, the NSGA-II is used as the solution methodology. In this way, the group average method is adopted to find the best solution from the Pareto front.

Therefore, to solve the non-linear multi-objective CEPDP, NSGA-II is adopted. This algorithm is one of the most significant and powerful heuristic algorithms to solve multi-objective optimization problems.

Running the NSGA-II, first of all, two populations are combined $(P_t \cup Q_t)$ to form a new population R_t with size 2 N. Afterward, the R_t is sorted into non-domination order. The approach ensures the elitism because all members of current and past populations are included in R_t. Currently, the set F_1 includes the best solutions in the population R_t. In this state, if condition *size(F1) < N* meets, then all members of the set F1 are selected for the next population P_{t+1}. The other members of the population P_{t+1} should be selected from subsequent non-dominated fronts. In continue, solutions from the

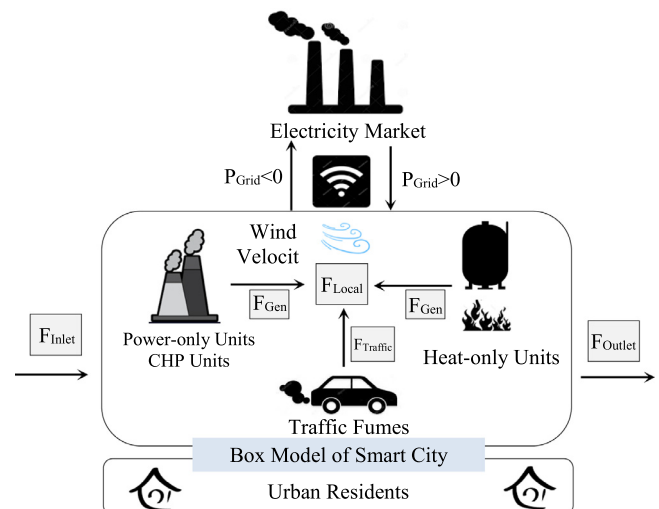**Fig. 2.** The Box model of air pollution for an urban area.

Fig. 3. Schematic diagram of the suggested smart city addressing pollution from local generation, traffic fumes and inlet/outlet volume.

set F_2 are selected followed by solutions from the set F_3. This procedure is iterated to cover all the sets ensuring no further sets can be evaluated [2]. The selection of one answer from a set of answers would be an arduous task for most of the decision-makers. Clustering, group average, central method, distance from ideal, quality criterion, dispersion criterion, and diversity criterion are some of the methods used to optimize a single answer. In this study, to select an answer from the Pareto front, the group average method is used. The procedure of NSGA II is described in Fig. 4.

To sum up, the flowchart of the coordination mechanism by the city operator is described in Fig. 5.

3. Numerical studies

In this section, the suggested approach is implemented in the test city. In the next subsections, first of all, the input data is illustrated. Afterward, the simulation results are presented and discussed.

3.1. Input data

In order to show the applicability of the proposed approach, the city of Semnan located in the center of Iran is considered as the test city. The maximum allowed capacity threshold for local pollution is equal to 2.6 mg/m^2 for every hour during the day. Note that the problem is based on bi-hourly operation scheduling. Characteristics of wind speed, heat, and power demands are described in Table 2.

The city consists of four power-only units, two CHP units, and one heat-only unit. Coefficients of cost function and allowed capacity threshold of generation units are described in the Appendix, Table A1. Fig. 6 shows the location of the test city with two tile lines to the main grid. Note that the test city can trade deficit/excess of energy through the tie lines in the electricity market.

The Feasible Operation Region (FOR) of power-heat function is illustrated in Fig. 7(a)-(b) for two CHP units.

In order to describe the price behavior in the electricity market, seasonal Auto-Regressive Integrated Moving Average, SARIMA $(1,0,1) \times (1,1,1)_{24}$ is used to generate scenarios for electricity price. The initial number of generated scenarios for the day-ahead market price is 50 and 1200 for one hour and one day, respectively. A large number of original total price scenarios increase the computational time burden of the problem noticeably. Therefore, to reduce the computational burden and achieve tractability, the size of scenarios is reduced through the Kantorovich distance function. As a result, the number of scenarios is reduced to 10 and 240 scenarios for one hour and the whole day, respectively [28]. The scenarios associated with a day-ahead electricity price of the main
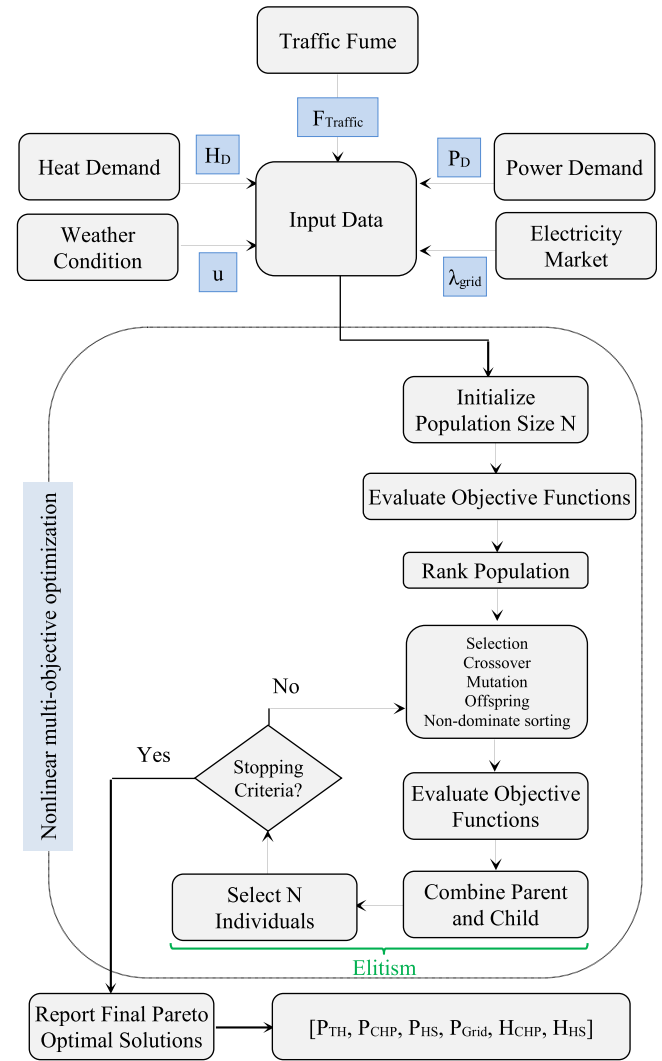

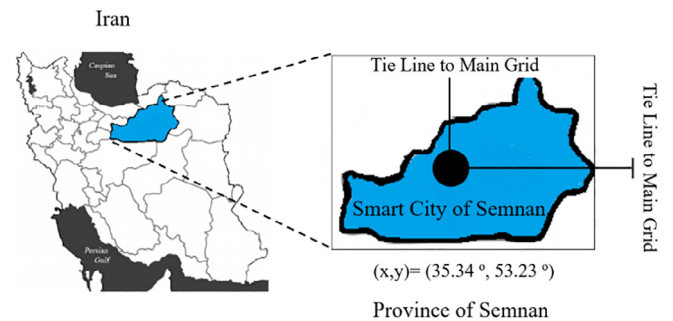**Fig. 5.** Flowchart of suggested approach.

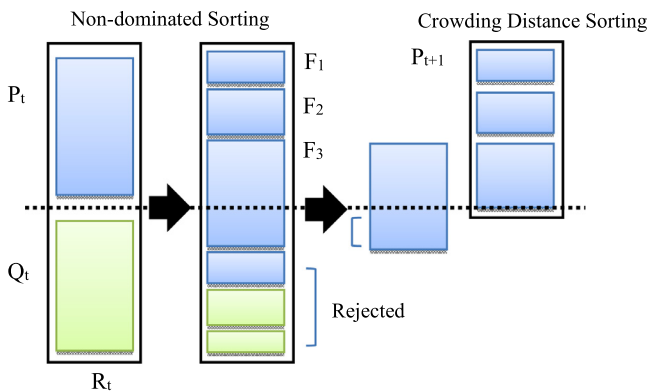**Fig. 6.** Location of the smart city of Semnan in the center of Iran.

grid is illustrated in Fig. 8. Finally, the daily profile of local traffic fume is described in Fig. 9. The input data of traffic fumes is extracted from local meteorological office.

3.2. Results and discussions

The CEPDP is formulated as a multi-objective problem which is solved using the NSGA II approach with MATLAB 9.1 software on

Fig. 4. Schematic diagram about the fundamentals of NSGA II.

Fig. 7. Feasible Operation Range of CHP units.
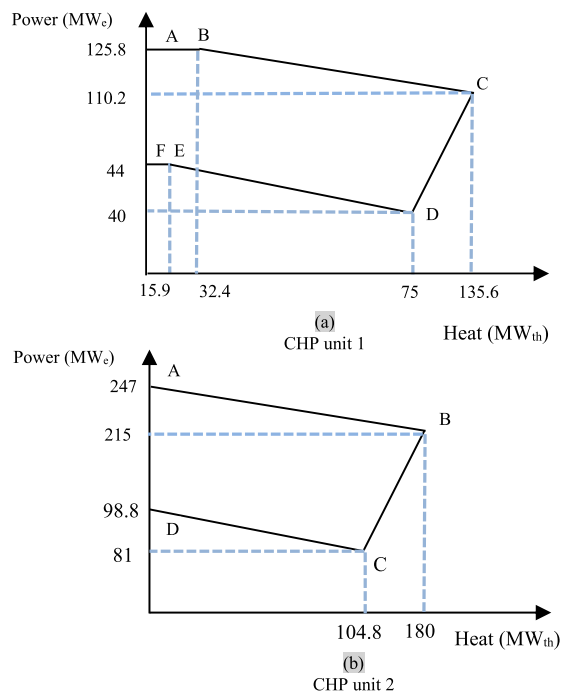
CHP 1 (a)

$P_{CHP}^1 - 125.8 \le 0$	$0 \le H_{CHP}^1 \le 32.4$
$P_{CHP}^1 + 0.151H_{CHP}^1 - 130.69 \le 0$	$32.4 \le H_{CHP}^1 \le 135.6$
$P_{CHP}^1 - 1.15H_{CHP}^1 - 45.74 \ge 0$	$75 \le H_{CHP}^1 \le 135.6$
$P_{CHP}^1 - 0.067H_{CHP}^1 - 45.02 \ge 0$	$15.9 \le H_{CHP}^1 \le 75$
$P_{CHP}^1 - 44 \ge 0$	$0 \le H_{CHP}^1 \le 15.9$

CHP 2 (b)

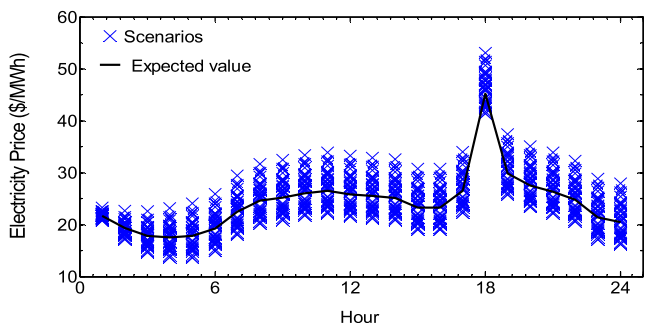|	
$P_{CHP}^2 + 0.177H_{CHP}^2 - 247 \le 0$	$0 \le H_{CHP}^2 \le 180$
$P_{CHP}^2 - 1.78H_{CHP}^2 + 105.4 \ge 0$	$104.8 \le H_{CHP}^2 \le 180$
$P_{CHP}^2 + 0.169H_{CHP}^2 - 99.08 \ge 0$	$0 \le H_{CHP}^2 \le 104.8$

Fig. 8. Scenarios of day-ahead electricity price.

Intel Pentium CPU at 1.6 GHz and 4 GB of RAM. In order to make a comparison between different states, three case studies are addressed. The main characteristics of case studies are described in Table 3. In brief, case study 1 investigates the optimum point from both cost and pollution objectives. In contrast, case study 2 finds the optimum point from the pollution objectives viewpoint. Finally, in case study 3, the role of the wind regime on the operation of the city is evaluated. In this case, both cost and pollution objectives are addressed.
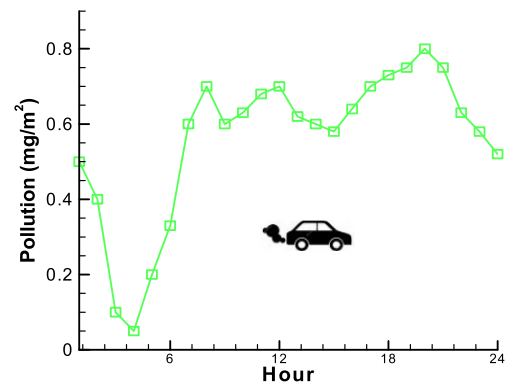

Fig. 9. Daily profile of local traffic fume.

3.2.1. Case study 1

In this case study, the CEPDP is fully optimized based on the information presented in Table 2. Fig. 10(a)-(b) show the generation level of power-only units, heat-only units, and cogeneration units. In addition, the distribution of local pollution for the 24-hour duration is illustrated in Fig. 11. In this figure, the cumulative local pollution from both local generation units and local traffic fumes is illustrated.

As the graph of generation level reveals, the generation of electrical energy increases considerably between 8 am and 16 pm when the electrical demand increases and the wind speed experiences an increase from 5 m/s to 7 m/s at the same time.

Considering Figs. 10 and 11, as the heat and power demands increase, and the wind speed reduces simultaneously, the concentration of pollutants in the city increases and reaches its maximum allowed threshold. In this situation, a sudden reduction in power and heat generations occurs to satisfy the maximum allowed threshold of pollution level. Therefore, the city is unable to meet the heat and power demands of local consumers in critical hours of the day (between 4:00 pm and 8:00 pm) in the islanded operation. In this situation, the city has to purchase the deficit of electrical demand from the main grid. It is evident that if the generation units do not decrease the generation level in the critical hours, the local pollution exceeds the maximum allowed threshold of pollution level. One interesting result is that the heavy traffic between 4:00 pm and 8:00 pm changes the operation of the city in terms of a local generation because the city has to meet the pollution constraints. Based on the graph, the local pollution from the local generation units coincides perfectly with the local pollution from traffic fumes (see Fig. 9). This issue shows how the local pollution from local generation and traffic fumes can change the optimum energy management strategies of a city. This issue is missed in the previous studies where the global emission was conventionally discussed.

Purchasing energy from the main grid, the cost of energy procurement from the main grid plus the cost of heat extraction from the available electrical energy should be added to the overall operation cost of the city in the critical hours. Fig. 12(a) and (b) describe the deficit/surplus of electrical and heat energies in the city, respectively. Obviously, the deficit/surplus of electrical energy should be purchased/sold from/to the electricity market. On the other hand, the deficit of heat energy should be extracted from electrical energy. Based on Fig. 12(a), the city purchases the most electrical energy from the main grid in critical hours when the electrical demand approaches the peak point and the concentration of local pollution reaches the maximum allowed threshold. The power transmitted between the city and the main grid reaches the lowest point in the remaining hours of the day.

Regarding the Fig. 12(b), we can say that the maximum heat shortage occurs in the critical hours while the city experiences
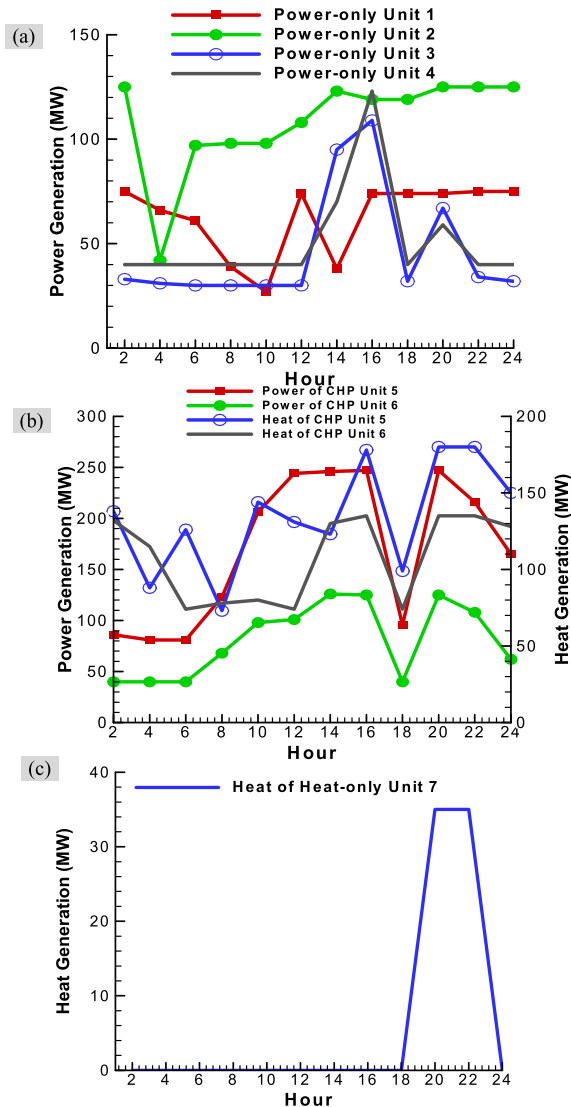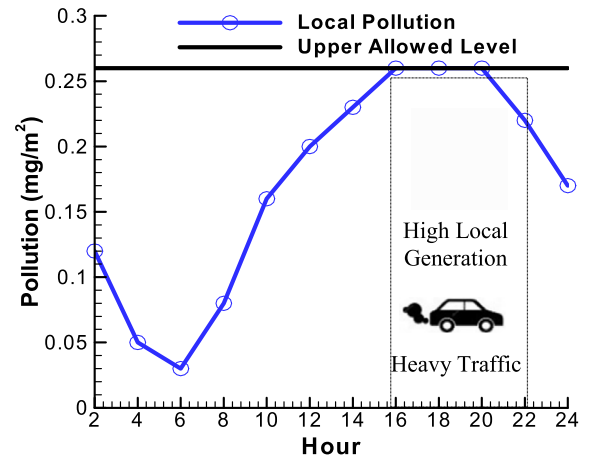
Table 2
Characteristics of wind speed, power and heat demands

Hour	2	4	6	8	10	12	14	16	18	20	22	24
P_d (MW)	400	300	350	400	500	600	700	800	900	800	600	500
H_d (MWt)	250	200	200	150	150	150	250	350	400	500	350	300
u_w (m/s)	2	3	4	5	6	7	6	5.2	4	3	2	2

Table 3
Description of three case studies

Case Study	Objective Function	Main Aim
1	$Min\left[F_{Operation}^{Cost}(t) + F_{Generation}^{Pollution}(t)\right]$	Optimize energy management strategies in terms of cost and local emission
2	$Min\left[F_{Generation}^{Pollution}(t)\right]$	Optimize energy management strategies subject to minimum local emission
3	$Min\left[F_{Operation}^{Cost}(t) + F_{Generation}^{Pollution}(t)\right]$	Evaluation of wind regime on the energy management strategies.

Fig. 11. Cumulative local pollution in the city from generation units and traffic fumes for Case Study 1.

Fig. 10. Optimized operation of generation units for Case Study 1 including (a) power-only (b) CHP and (c) heat-only units.
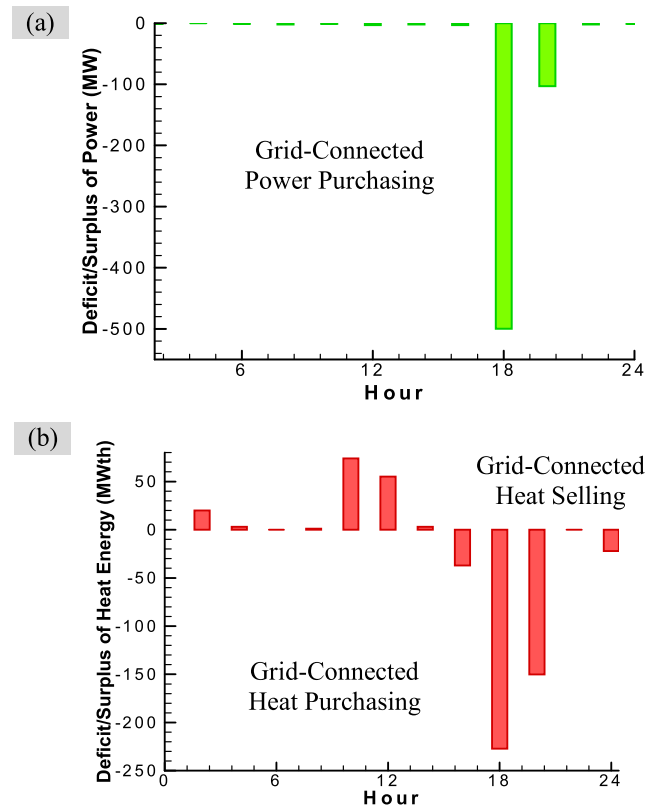
Fig. 12. Power/heat traded between city and main grid for Case Study 1.

the overproduction of heat energy in the remaining hours. Note that in the CEPDP for different generation units, the co-generation units are in priority. This means that each variation in electrical and/or heat demand should be compensated by increas-

ing and/or decreasing in the generation of CHP units as much as possible. The other generation units are in the next priorities.

3.2.2. Case study 2

In case study 2, in order to choose an answer from the Pareto front, the best answer from the viewpoint of pollution function is used. In fact, in this case study, the problem is optimized based on the pollution function while the cost function of the city is not optimized in the problem. Consequently, the economic aspect of the problem is omitted and the pollution aspect of the problem is emphasized. Fig. 13 shows the Pareto front considering the pollution function versus cost, solved by NSGA II in MATLAB software. The general optimum point is found considering both the economy and pollution objectives. However, in this case study, in order to investigate the role of pollution in the problem, the best answer with respect to pollution objective is selected from the Pareto front (the lowest right point).

Fig. 14 describes the generation levels for different generation units of the city. Comparing the Figs. 10 and 14, we can say that the power-only units generate more electrical energy in critical hours in case study 2 in contrast to case study 1. Actually, we cannot see any valley in the generation profile of the power-only units for case study 2, especially in the critical hours when the power-only units experience deep valleys in the case study 1. In contrast, the CHP and heat-only units experience deep valleys in the critical hours for heat energy generation. The reason is that the problem is optimized emphasizing the pollution function with no considering the cost function.

Fig. 15 describes the pollution level of the city for case study 2. As the graph reveals, choosing the best answer from the Pareto front with considering the pollution function only leads to a significant reduction in the local pollutant production. In this way, the concentration of the pollutant approaches the maximum allowed threshold in critical hours without exceeding it. It is important to know that this solution is not only cost-effective but also increases both power generation costs from power-only units and power procurement cost from the main grid.

Fig. 16(a) and (b) illustrate the deficit/surplus of generated energy for electrical and heat energies, respectively. As the graphs reveal, the most shortage of heat and power energies occurs in the critical hours. As a result, the city operator has to purchase more electrical energy from the main grid to satisfy the electrical and heat demands of end-use consumers.

Fig. 17 compares the values of pollution and cost functions of the city for case studies 1 and 2. Based on the line graph, we can say that the operation cost of the city increases while the pollution function values of the problem decrease in case study 2 in comparison with the case study 1.
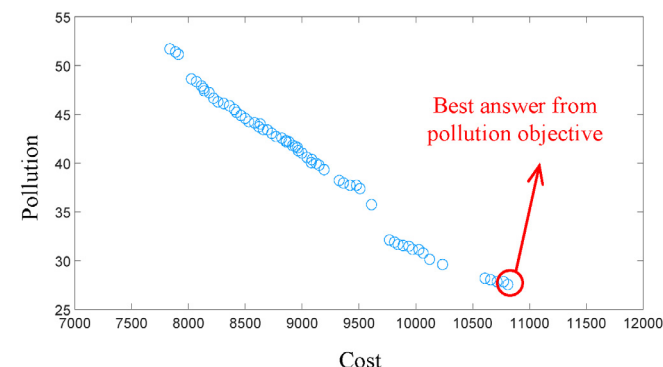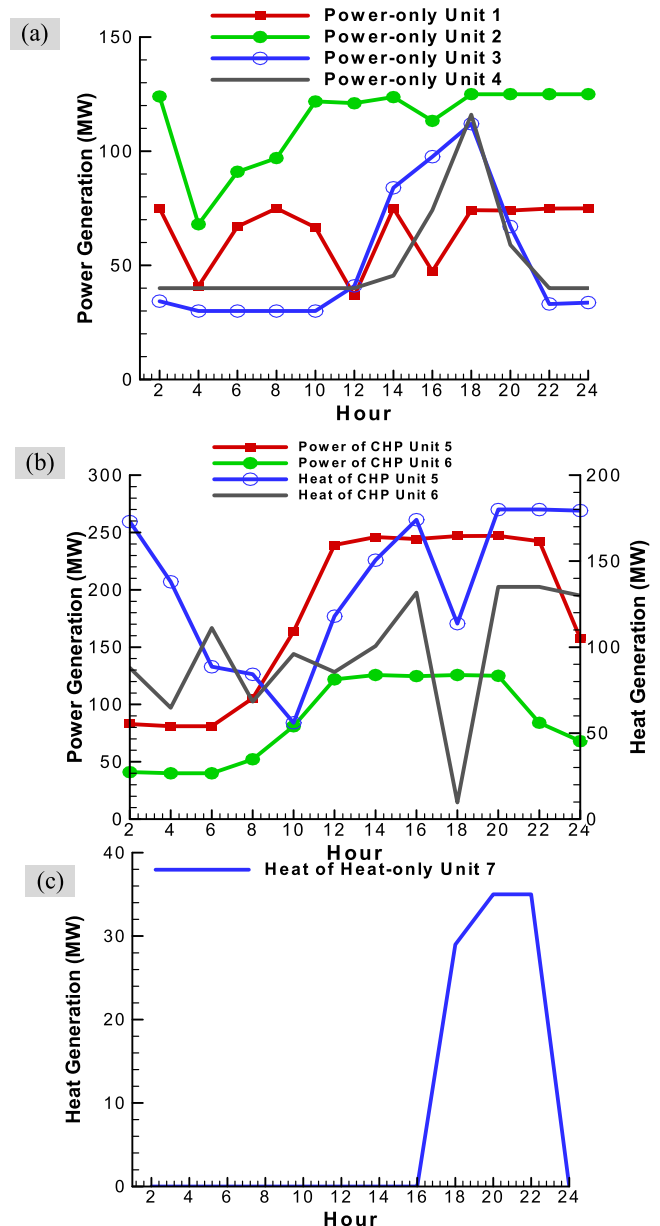
Fig. 14. Optimized operation of generation units for Case Study 2 including (a) power-only (b) CHP and (c) heat-only units.

3.2.3. Case study 3

In case study 3, to evaluate the impacts of the wind speed regime on pollutants' evacuation rate in the urban city, the speed values of wind regime were decreased to the half of those presented in the case study 1 (Table 2). Fig. 18 describes the pollution generation data comparing the results for case studies 1 and 3. Based on the graph, we can say that as the wind speed decreases, the concentration of pollutants increases considerably and reaches the maximum allowed threshold at around 12 am. In this situation, in order to meet the maximum allowed threshold for pollution level, the city operators have to decrease the production levels of generation units. Consequently, to satisfy the electrical and heat demands of the end-use consumers, the city should purchase more electrical energy from the main grid with high procurement cost.

To sum up, it is obvious that integrating distributed generation to urban areas increases the efficiency of the power systems. However, this approach transmits the pollutants from suburban areas to the urban ones; consequently, it can cause health problems for
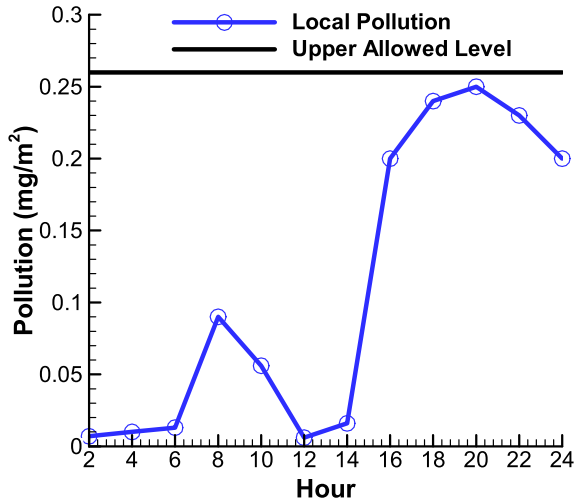
Fig. 13. Pareto front-optimized values of the objective functions: pollution versus cost.

Fig. 15. Local pollution in the city from generation units and traffic fumes for Case Study 2.
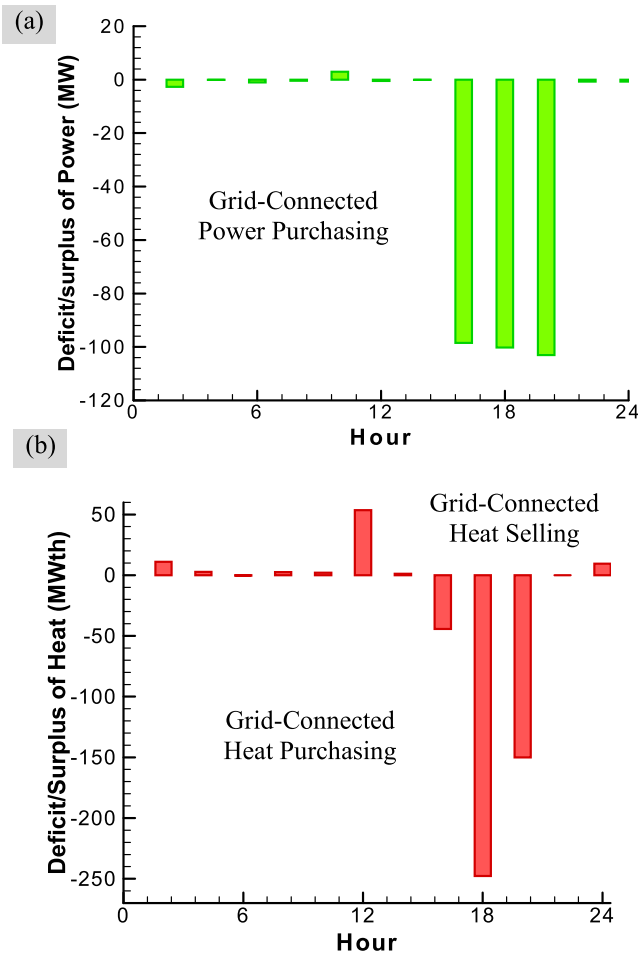
Fig. 16. Power/heat traded between smart city and main grid for Case Study 2.

Fig. 17. Comparison of objective values for cost and pollution functions in Case Studies 1 and 2.

Fig. 18. Comparison of local pollution in the city between Case Studies 1 and 3.

4. Conclusion

In this paper, the economic pollution dispatch problem for an urban area is presented to determine optimized operation scheduling of the smart city under local pollution constraints. The problem is formulated through a multi-objective problem which is solved by the NSGA II approach.

The results show that when the optimum point is found considering both cost and pollution objectives, the power and heat production of all generation units experience a significant reduction in high demand hours. In fact, the local pollution objectives reduce the generation output to meet the local pollution constraint. Therefore, the city purchases the deficit of energy from the upstream market. In contrast, when the cost objective is omitted from the Pareto front, the operation cost of the city increases significantly. Instead, the concentration of local pollution reduces considerably.

Moreover, it is observed that if the wind speed decreases, the concentration of pollutants in the air of the city increases. Consequently, to prevent from exceeding the local pollution constraint, especially in the hours with heavy car traffic, the city has to decrease the generation level and procure the required energy from the main grid. The interesting result is that the traffic fumes

the residents of cities. For this reason, in order to perform a comprehensive study about the operation of distributed generation in an urban city, it is essential to consider the constraints of air pollution in the problem. In fact, this makes it possible to strike the right balance between the operation cost and a healthy lifestyle.
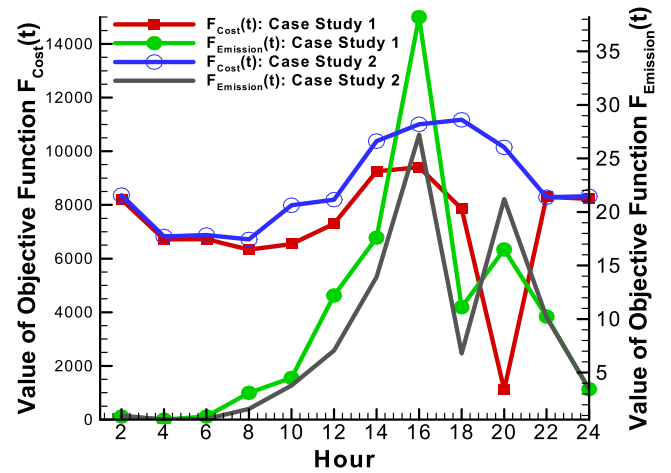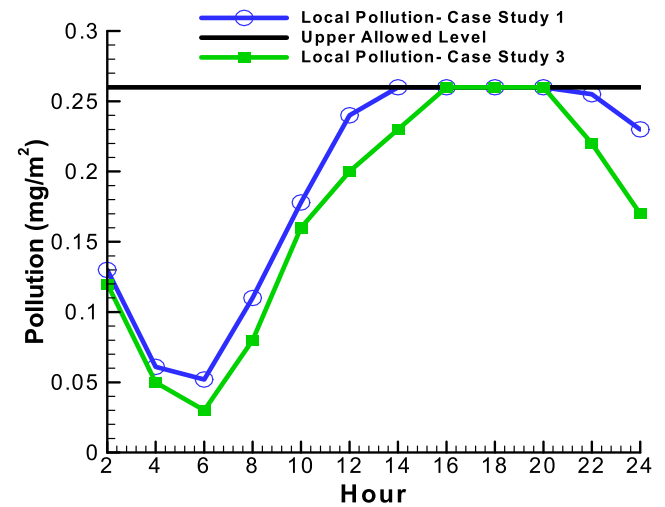
in the hours with heavy car traffic change the operation of the distributed generation to meet the pollution constraint.

It is confirmed that although the distributed generation in cities decreases the global emission, it increases the local pollution in some time durations; therefore, it can deviate the operation of local generation from the optimum economic point. Therefore, urban energy generation can transmit the pollutants from the sub-urban areas to the urban ones. To sum up, the energy management of distributed generation in urban areas should be investigated considering the local air pollution.

Declaration of Competing Interest

The authors declare that they have no known competing financial interests or personal relationships that could have appeared to influence the work reported in this paper.

Appendix

Table A1
Technical data of generation units

No.	Type	Cost Function	Capacity (MW)
1	Power-only	$F_{TH}^1(t) = 25 + 2P_{TH}^1(t) + 0.008(P_{TH}^1(t))^2 + |100.\sin[0.042(P_{TH,\,min}^1(t) - P_{TH}^1(t))]|$	$10 \leq P_1 \leq 75$
2	Power-only	$F_{TH}^2(t) = 60 + 1.8P_{TH}^2(t) + 0.003(P_{TH}^2(t))^2 + |140.\sin[0.04(P_{TH,\,min}^2(t) - P_{TH}^2(t))]|$	$20 \leq P_2 \leq 125$
3	Power-only	$F_{TH}^3(t) = 100 + 2.1P_{TH}^3(t) + 0.001(P_{TH}^3(t))^2 + |160.\sin[0.038(P_{TH,\,min}^3(t) - P_{TH}^3(t))]|$	$30 \leq P_3 \leq 175$
4	Power-only	$F_{TH}^4(t) = 120 + 2P_{TH}^4(t) + 0.001(P_{TH}^4(t))^2 + |180.\sin[0.037(P_{TH,\,min}^4(t) - P_{TH}^4(t))]|$	$40 \leq P_4 \leq 250$
5	CHP	$F_{CHP}^5(t) = 2650 + 14.5P_{CHP}^5(t) + 0.0345(P_{CHP}^5(t))^2 + 4.2H_{CHP}^5(t) + 0.03(H_{CHP}^5(t))^2 + 0.031P_{CHP}^5(t).H_{CHP}^5(t)$	FOR- Fig. 7
6	CHP	$F_{CHP}^6(t) = 1250 + 36P_{CHP}^6(t) + 0.0435(P_{CHP}^6(t))^2 + 0.9H_{CHP}^6(t) + 0.027(H_{CHP}^6(t))^2 + 0.11P_{CHP}^6(t).H_{CHP}^6(t)$	FOR- Fig. 7
7	Heat-only	$F_{HS}^7(t) = 950 + 2.0109H_{HS}^k(t) + 0.038\left(H_{HS}^k(t)\right)^2$	$0 \leq H_7 \leq 2695.2$

References

[1] H. Golmohamadi, R. Keypour, Application of robust optimization approach to determine optimal retail electricity price in presence of intermittent and conventional distributed generation considering demand response, J. Control Autom. Electr. Syst. 28 (5) (2017) 664–678.

[2] R.J. Flores, J. Brouwer, Optimal design of a distributed energy resource system that economically reduces carbon emissions, Appl. Energy 232 (2018) 119–138.

[3] H. Golmohamadi, R. Keypour, B. Bak-Jensen, J. Radhakrishna Pillai, Optimization of household energy consumption towards day-ahead retail electricity price in home energy management systems, Sustainable Cities and Society 47 (2019), https://doi.org/10.1016/j.scs.2019.101468.

[4] H. Golmohamadi, R. Keypour, A bi-level robust optimization model to determine retail electricity price in presence of a significant number of invisible solar sites, Sustainable Energy Grids Networks 13 (2018) 93–111.

[5] A. Farag, S. Al-Baiyat, T. Cheng, Economic load dispatch multiobjective optimization procedures using linear programming techniques, IEEE Trans. Power Syst. 10 (2) (1995) 731–738.

[6] S.J.P.S. Mariano, J.P.S. Catalao, V.M.F. Mendes, L.A.F.M. Ferreira, Profit-based short-term hydro scheduling considering head-dependent power generation, IEEE Lausanne Power Tech, Lausanne, Switzerland, 2007.

[7] G.W. Chang, M. Aganagic, J.G. Waight, J. Medina, Experiences with mixed integer linear programming based approaches on short-term hydro scheduling, IEEE Trans. Power Syst. 16 (4) (2001) 743–749.

[8] S.-C. Chang, C.-H. Chen, I.-K. Fong, P. Luh, Hydroelectric generation scheduling with an effective differential dynamic programming algorithm, IEEE Trans. Power Syst. 5 (3) (1990) 737–743.

[9] V.S. Kumar, M.R. Mohan, A genetic algorithm solution to the optimal short-term hydrothermal scheduling, Int. J. Electr. Power Energy Syst. 33 (4) (2011) 827–835.

[10] E.B. Schlünz, J.H. van Vuuren, An investigation into the effectiveness of simulated annealing as a solution approach for the generator maintenance scheduling problem, Int. J. Electr. Power Energy Syst. 53 (2013) 166–174.

[11] J. Zhou, C. Wang, Y. Li, P. Wang, C. Li, P. Lu, Li. Mo, A multi-objective multi-population ant colony optimization for economic emission dispatch considering power system security, Appl. Math. Model. 45 (2017) 684–704.

[12] X. Chen, B. Xu, W. Du, An improved particle swarm optimization with biogeography-based learning strategy for economic dispatch problems, Complexity 2018 (2019) 1–15.

[13] A. Chatterjee, S.P. Ghoshal, V. Mukherjee, Solution of combined economic and emission dispatch problems of power systems by an opposition-based harmony search algorithm, Int. J. Electr. Power Energy Syst. 39 (1) (2012) 9–20.

[14] S.D. Beigvand, H. Abdi, M. La Scala, Combined heat and power economic dispatch problem using gravitational search algorithm, Electr. Power Syst. Res. 133 (2016) 160–172.

[15] Economic and Emission Dispatch Using Ensemble Multi-Objective Differential Evolution Algorithm,'' Sustainability, 10(2), 2018.

[16] M. Jevtić1, N. Jovanović, J. Radosavljević, Solving a combined economic emission dispatch problem using adaptive wind driven optimization, Turkish J. Electr. Eng. Computer Sci. 26 (2018) 1747–1758.

[17] T. Cheng, M. Chen, Adaptive robust method for dynamic economic emission dispatch incorporating renewable energy and energy storage, Complexity 2018 (2018) 1–13.

[18] T. Deng, X. He, Z. Zeng, Recurrent neural network for combined economic and emission dispatch, Appl. Intell. 48 (8) (2018) 2180–2198.

[19] Z. Li, W. Wu, M. Shahidehpour, Combined heat and power dispatch considering pipeline energy storage of district heating network, IEEE Trans. Sustain. Energy 7 (1) (2016) 12–22.

[20] C. Lin, W. Wu, B. Zhang, Y. Sun, Decentralized Solution for combined heat and power dispatch through benders decomposition, IEEE Trans. Sustainable Energy 8 (4) (2017) 1361–1372.

[21] A.Y. Abdelaziz, E.S. Ali, S.M. Abd Elazim, Flower pollination algorithm to solve combined economic and emission dispatch problems, Eng. Sci. Technol., Int. J. 19 (2) (2016) 980–990.

[22] Z. Hu, M. Zhang, X. Wang, Chen Li, M. Hu, Bi-level robust dynamic economic emission dispatch considering wind power uncertainty, Electr. Power Syst. Res. 135 (2016) 35–47.

[23] G. Liu, Y.L. Zhu, W. Jiang, Wind-thermal dynamic economic emission dispatch with a hybrid multi-objective algorithm based on wind speed statistical analysis, IET Gener. Transm. Distrib. 12 (17) (2018) 3972–3984.

[24] M.-T. Kuo, S.-D. Lu, M.-C. Tsou, Considering carbon emissions in economic dispatch planning for isolated power systems: a case study of the Taiwan power system, IEEE Trans. Ind. Applicat. 54 (2) (2018) 987–997.

[25] H. Liang, Y. Liu, F. Li, Y. Shen, Dynamic economic/emission dispatch including PEVs for peak shaving and valley filling, IEEE Trans. Ind. Electron. 66 (4) (2019) 2880–2890.

[26] M.S. Ahmad, S. Sivasubramani, Optimal number of electric vehicles for existing networks considering economic and emission dispatch, IEEE Trans. Ind. Inf. 15 (4) (2019) 1926–1935.

[27] T. Goh, B.W. Ang, X.Y. Xu, Quantifying drivers of CO2 emissions from electricity generation – Current practices and future extensions, Appl. Energy 231 (2018) 1191–1204.

[28] D. Quiroga, E. Sauma, D. Pozo, Power system expansion planning under global and local emission mitigation policies, Appl. Energy 239 (2019) 1250–1264.

[29] M. Nazari-Heris, B. Mohammadi-Ivatloo, G.B. Gharehpetian, A comprehensive review of heuristic optimization algorithms for optimal combined heat and power dispatch from economic and environmental perspectives, Renew. Sustain. Energy Rev. 81 (2018) 2128–2143.

[30] Y.a. Shaabani, A.R. Seifi, M.J. Kouhanjani, Stochastic multi-objective optimization of combined heat and power economic/emission dispatch, Energy 141 (2017) 1892–1904.

[31] M.J. Kim, T.S. Kim, R.J. Flores, J. Brouwer, Neural-network-based optimization for economic dispatch of combined heat and power systems, Appl. Energy 265 (2020).

[32] X. Shen, D. Zou, N. Duan, Q. Zhang, An efficient fitness-based differential evolution algorithm and a constraint handling technique for dynamic economic emission dispatch, Energy 186 (2019).

[33] E.E. Elattar, Modified harmony search algorithm for combined economic emission dispatch of microgrid incorporating renewable sources, Energy 159 (2018) 496–507.

[34] T. Niknam, R. Azizipanah-Abarghooee, A. Roosta, B. Amiri, A new multi-objective reserve constrained combined heat and power dynamic economic emission dispatch, Energy 42 (1) (2012) 530–545.

[35] G.S. Piperagkas, A.G. Anastasiadis, N.D. Hatziargyriou, Stochastic PSO-based heat and power dispatch under environmental constraints incorporating CHP and wind power units, Electr. Power Syst. Res. 81 (1) (2011) 209–218.

[36] M. Basu, Bee colony optimization for combined heat and power economic dispatch, Expert Syst. Appl. 38 (11) (2011) 13527–13531.

[37] A. Rong, H. Hakonen, R. Lahdelma, A dynamic regrouping based sequential dynamic programming algorithm for unit commitment of combined heat and power systems, Energy Convers. Manage. 50 (4) (2009) 1108–1115.